1.D.1 *Nuclear Physics* **56** (1964) 548—568;

SHELL MODEL CALCULATIONS ON ENERGY LEVELS IN THE $2s_{\frac{1}{2}}\,1d_{\frac{3}{2}}$ SHELL (II)

P. W. M. GLAUDEMANS, G. WIECHERS † and P. J. BRUSSAARD

Fysisch Laboratorium der Rijksuniversiteit, Utrecht, The Netherlands

Received 10 February 1964

Abstract: Shell model calculations on nuclei in the region $28 < A \leq 40$ are performed with the assumption of an inert ^{28}Si core. The theory underlying these calculations has been described in an earlier paper. The numerical results are presented here. The values of the two-particle interactions in the $2s_{\frac{1}{2}}\,1d_{\frac{3}{2}}$ shell and the binding energies to the ^{28}Si core of $2s_{\frac{1}{2}}$ and $1d_{\frac{3}{2}}$ particles are derived from experimental level energies. The calculated energies, spins and configurations of about 400 levels are listed. With the nuclear wave functions obtained, the spectroscopic factors for stripping reactions are calculated and, where possible, compared with the experimental data.

1. Introduction

In a previous paper [1]) (in the following referred to as I) it was shown that all (two-particle) interactions between nucleons in the various configurations of the $2s_{\frac{1}{2}}\,1d_{\frac{3}{2}}$ shell can be expressed in terms of fifteen interaction energies of two-particle configurations. With the binding energies (to the ^{28}Si core) of a nucleon in the $2s_{\frac{1}{2}}$ shell and in the $1d_{\frac{3}{2}}$ shell one thus obtains seventeen parameters in terms of which the interaction matrix elements of the nuclear Hamiltonian can be expressed. Most of the necessary two-particle interactions are diagonal; however, some non-diagonal interactions are also needed to evaluate the mixing between states of different configurations, but with the same spin and isospin. The best values of the seventeen parameters are obtained from a least-squares fitting procedure, in which computed energies are compared with energies of a number of states with experimentally well-known spin and isospin. This requires linearization and iteration processes, also described in paper I.

A tentative set of the parameters was obtained by a preliminary inspection of the experimental data and comparison with Arima's results [2]). For the first run on the computer only the energies of ground states and a few first excited states were utilized. With the parameters obtained in this way, the energies of more states were computed and compared with experiment. Some of these states were selected and taken along in the next computer run. This process was repeated several times. Altogether fifty states were taken along in the final fitting procedure.

With the values of the parameters thus obtained, the energies and wave functions

† Present address: Department of Physics, University of Cape Town, South Africa.

of all the 377 states in the $2s_{\frac{1}{2}}1d_{\frac{3}{2}}$ shell were calculated (sect. 2). Finally, these wave functions were used to compute reduced widths for some stripping reactions in the region $28 \leqq A < 40$ (sect. 3).

All calculations (except the first trial runs on the ZEBRA computer of the Utrecht Mathematical Institute) were performed with the X1 electronic computer at the Amsterdam Mathematical Center.

2. Results

2.1. VALUES OF THE PARAMETERS

The fifty states used for the determination of the parameters are indicated in figs. 2–5 by bold lines. The average of the absolute values of the deviations between the experimental and computed energies amounts to 0.11 MeV. The numerical results were obtained in five cycles of the iteration process (i.e., after the fifty states had been selected). Each cycle took about three hours on the X1 computer.

TABLE 1

Parameter values (in MeV)			
$\langle s^2\|H\|s^2\rangle$	0,1 = −1.351		
$\langle s^2\|H\|s^2\rangle$	1,0 = −2.403		
$\langle d^2\|H\|d^2\rangle$	0,1 = −2.277		
$\langle d^2\|H\|d^2\rangle$	2,1 = +0.159		
$\langle d^2\|H\|d^2\rangle$	1,0 = −0.916		
$\langle d^2\|H\|d^2\rangle$	3,0 = −2.644		
$\langle sd\|H\|sd\rangle$	1,1 = +1.792	B_0	= −0.524
$\langle sd\|H\|sd\rangle$	2,1 = −1.006	B_j	= −0.724
$\langle sd\|H\|sd\rangle$	1,0 = −3.857	B_t	= +2.267
$\langle sd\|H\|sd\rangle$	2,0 = −1.246	B_{jt}	= −2.706
$\langle s^2\|H\|d^2\rangle$	0,1 = +1.493		
$\langle s^2\|H\|sd\rangle$	1,0 = −0.205		
$\langle s^2\|H\|d^2\rangle$	1,0 = +0.039		
$\langle sd\|H\|d^2\rangle$	1,0 = −0.511		
$\langle sd\|H\|d^2\rangle$	2,1 = +0.441		
E_s	= −8.391		
E_d	= −7.173		

The values of the fifteen two-particle interactions of the $2s_{\frac{1}{2}}$ $1d_{\frac{3}{2}}$ shell (denoted by $\langle \rho\rho'|H|\rho''\rho'''\rangle JT$), and the binding energies of a nucleon in the $2s_{\frac{1}{2}}$ and $1d_{\frac{3}{2}}$ shell (E_s and E_d, respectively). The coefficients B_0, B_j, B_t and B_{jt} are specific linear combinations (see I) of the four diagonal two-particle interactions in the sd configuration.

Table 1 shows the two-particle interaction energies for the two s^2 configurations, the four d^2 configurations and the four sd configurations. The latter four have been found from the values of B_0, B_j, B_t and B_{jt}, which have been used in the actual calculations [cf., I eq. (4.13)]. Furthermore the non-diagonal two-particle interactions are given. The values E_s and E_d represent the binding energies to the core of an $s_{\frac{1}{2}}$ and a $d_{\frac{3}{2}}$ particle, respectively.

It follows from table 1 that two particles in an sd configuration coupled to $J = 1$, $T = 0$, show the strongest attractive force ($E = -3.857$ MeV), whereas two particles in the same configuration coupled to $J = 1$, $T = 1$, repel each other most strongly ($E = +1.792$ MeV).

2.2. BINDING ENERGIES

In fig. 1 the differences between the calculated and experimental ground-state binding energies are given for $28 < A \leqq 40$. The binding energies are reproduced to within 0.15 MeV in most cases. Exceptions are ^{36}Cl, ^{36}Ar, ^{37}Ar and ^{38}Ar. Other deviations

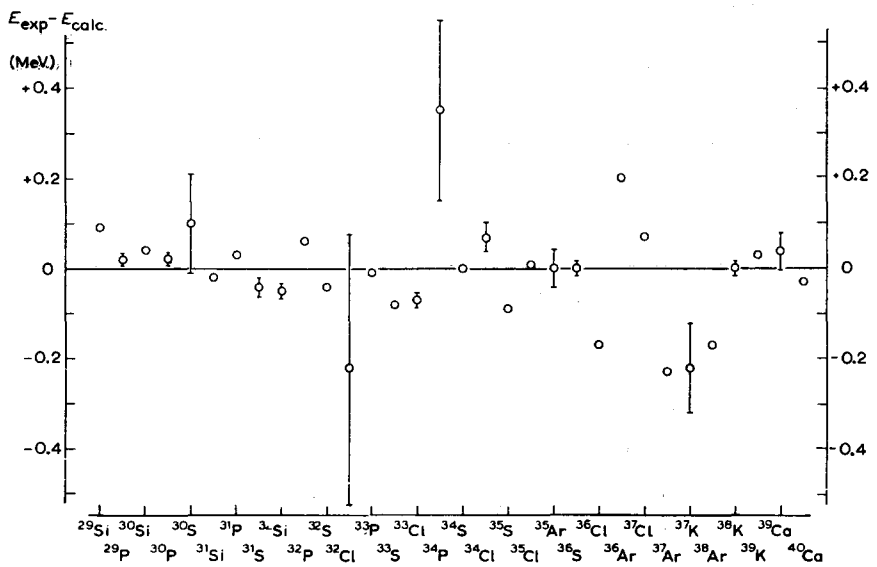

Fig. 1. Difference between experimental and calculated ground-state binding energies. The bars represent the experimental errors larger than 0.01 MeV.

larger than 0.15 MeV may be explained by uncertainties in the experimental values. The experimental binding energies are taken from ref. [3]), with improvements as given in ref. [4]).

2.3. ENERGY LEVELS

In table 2 the complete list of the calculated level energies, spins and configurations is given. Binding energies are given relative to the binding energy of the ^{28}Si core, with the Coulomb energy of all particles outside the core subtracted [1]).

Each matrix in the table is labelled by a heading indicating the mass number A, the chemical symbol and the pair of (J, T) values. Subheadings indicate the order of the energy matrix in question, the experimental binding energy of the ground state (see I, table 1; if a pair of nuclei is listed the value refers to the first nucleus, except for

TABLE 2

Calculated energies and configurations

29P/Si(1/2,1/2)

			s1
	1	- 8.44	11
+ .05	- 8.39	+1000	

29P/Si(3/2,1/2)

			d1
	1	- 8.44	21
+ 1.27	- 7.17	+1000	

30P(1,0)

			s2	s1d1	d2
	3	- 19.72	10	1131	10
+ .02	- 19.70	+232	+749	+ 19	
+ .69	- 19.03	-768	+222	+ 10	
+ 4.58	- 15.14	+ 0	- 28	+971	

30P(3,0)

			d2
	1	- 19.72	30
+ 2.73	- 16.99	+1000	

30P(2,0)

			s1d1
	1	- 19.72	1131
+ 2.91	- 16.81	+1000	

30P/Si(0,1)

			s2	d2
	2	- 19.72	01	01
+ .67	- 19.05	-726	+274	
+ 4.02	- 15.70	+274	+726	

30P/Si(2,1)

			s1d1	d2
	2	- 19.72	1131	21
+ 3.00	- 16.72	-943	+ 57	
+ 5.69	- 14.03	+ 57	+943	

30P/Si(1,1)

			s1d1
	1	- 19.72	1131
+ 5.95	- 13.77	+1000	

31P/S(1/2,1/2)

			s3	s2d1	s1d2	s1d2	d3
	5	- 32.00	11	1031	1101	1110	11
- .01	- 32.01	-675	+ 4	-288	- 27	+ 7	
+ 3.46	- 28.54	+311	+ 9	-473	-167	+ 40	
+ 6.35	- 25.65	+ 0	-950	- 33	+ 15	+ 1	
+ 8.85	- 23.15	- 14	- 24	+203	-487	+273	
+ 9.99	- 22.01	- 0	- 13	+ 3	-305	-679	

31P/S(3/2,1/2)

			s2d1	s2d1	s1d2	s1d2	d3
	5	- 32.00	0131	1031	1110	1121	21
+ 1.22	- 30.78	-640	-205	+ 9	+ 6	+141	
+ 3.27	- 28.73	- 1	- 26	+223	+489	-266	
+ 5.26	- 26.74	- 5	-303	- 55	-209	-428	
+ 7.25	- 24.75	+348	-468	+ 0	+ 23	+160	
+ 8.29	- 23.71	- 6	+ 0	-712	+278	- 3	

31P/S(5/2,1/2)

			s2d1	s1d2	s1d2	d3
	4	- 32.00	1031	1130	1121	21
+ 3.18	- 28.82	-874	+ 29	+ 96	- 0	
+ 5.60	- 26.40	+117	+449	+432	- 2	
+ 7.89	- 24.11	- 1	+ 77	- 41	+880	
+ 8.56	- 23.44	+ 8	-444	+431	+118	

31P/S(7/2,1/2)

			s1d2	d3
	2	- 32.00	1130	71
+ 4.15	- 27.85	-886	+114	
+ 7.09	- 24.91	+114	+886	

31Si(3/2,3/2)

			s2d1	s1d2	d3
	3	- 25.68	0131	1121	33
- .02	- 25.70	-871	+ 27	-102	
+ 3.65	- 22.05	+124	+ 56	-821	
+ 5.55	- 20.14	+ 5	+917	+ 77	

31Si(5/2,3/2)

			s1d2
	1	- 25.68	1121
+ 1.79	- 23.89	+1000	

31Si(1/2,3/2)

			s1d2
	1	- 25.68	1101
+ .76	- 24.93	+1000	

32Si(0,2)

			s2d2	d4
	2	- 35.00	0101	02
- .04	- 35.04	-914	- 86	
+ 5.28	- 29.72	- 86	+914	

32Si(2,2)

			s2d2	s1d3
	2	- 35.00	0121	1132
+ 2.45	- 32.55	-710	-290	
+ 5.85	- 31.17	-290	+710	

32Si(1,2)

			s1d3
	1	- 35.00	1132
+ 6.23	- 28.77	+1000	

For the meaning of the symbols used see subsect. 2.3.

TABLE 2 (continued)

32P/Cl(1,1)

	8	- 39.81	s3d1 s2d2 s2d2 s2d2 s1d3 s1d3 s1d3 d4 1131 1001 0110 1021 1111 1131 1133 11
-	.05	- 39.86	-574 +140 +109 - 30 + 38 + 0 +109 - 0
+	1.06	- 38.74	+267 +503 +157 - 10 + 9 - 33 - 13 + 9
+	2.13	- 37.68	+ 21 -126 + 23 - 41 + 10 -566 +212 + 1
+	3.30	- 36.50	+ 74 + 30 -124 + 44 +192 + 73 +380 - 81
+	4.57	- 35.24	+ 51 -172 +316 -123 + 51 +280 + 7 + 2
+	7.12	- 32.69	- 2 - 16 + 59 +522 + 99 - 1 - 0 +300
+	8.35	- 31.46	- 3 - 11 +137 +146 + 15 - 24 - 60 -606
+	9.13	- 30.68	- 7 - 2 - 76 - 85 +585 - 24 -219 + 1

32P/Cl(2,1)

	7	- 39.81	s3d1 s2d2 s2d2 s1d3 s1d3 s1d3 d4 1131 0121 1021 1131 1151 1133 21
-	.11	- 39.92	-729 + 59 - 1 +109 + 7 + 89 - 4
+	1.00	- 38.81	- 49 -536 -256 - 33 + 10 + 21 + 95
+	2.88	- 36.93	+141 - 30 - 1 +704 + 51 + 60 + 13
+	4.25	- 35.56	- 38 - 78 - 9 +144 -181 -481 - 69
+	4.98	- 34.83	- 30 - 2 +275 + 3 + 1 - 84 +605
+	7.37	- 32.44	- 9 -291 +450 - 6 + 16 + 40 -188
+	9.41	- 30.40	- 4 + 3 - 9 - 1 +733 -225 - 26

32P/Cl(3,1)

	5	- 39.81	s2d2 s2d2 s1d3 s1d3 d4 0130 1021 1151 1171 31
+	1.30	- 38.51	-618 -320 - 1 + 18 + 42
+	3.46	- 36.35	-222 +623 + 34 + 68 + 53
+	4.68	- 35.13	+ 0 + 22 -731 - 52 +196
+	6.27	- 33.54	-150 + 33 - 74 -142 -600
+	7.80	- 32.00	+ 10 - 1 -161 +720 -108

32P/Cl(0,1)

	2	- 39.81	s2d2 s1d3 0101 1111
+	.52	- 39.29	-982 + 18
+	9.99	- 29.81	+ 18 +982

32P/Cl(4,1)

	1	- 39.81	s1d3 1171
+	3.73	- 36.08	+1000

32S(2,0)

	8	- 47.06	s3d1 s2d2 s2d2 s2d2 s1d3 s1d3 d4 d4 1131 1030 1010 0121 1131 1151 20 20"
+	2.32	- 44.74	-689 + 7 - 5 + 28 -240 + 8 + 20 - 3
+	4.85	- 42.21	+ 1 - 55 +192 -509 -196 + 8 - 34 - 4
+	6.40	- 40.66	+267 + 14 + 0 + 63 -322 + 55 +267 - 11
+	9.75	- 37.31	- 35 - 42 +169 - 18 +129 - 14 +580 + 13
+	10.69	- 36.37	+ 0 +355 +489 + 71 - 0 - 42 - 40 + 2
+	12.09	- 34.97	- 7 + 83 + 6 - 15 + 95 +787 - 0 - 7
+	13.71	- 33.35	+ 0 +412 -135 -272 - 1 - 43 + 48 + 89
+	14.32	- 32.74	+ 1 - 32 + 4 + 22 - 15 + 43 - 10 +872

32S(0,0)

	5	- 47.06	s4 s2d2 s2d2 s1d3 d4 00 0101 1010 1111 00
-	.04	- 47.10	-496 +391 + 59 - 12 - 42
+	4.06	- 43.00	+468 +242 + 92 - 12 -186
+	5.90	- 41.16	+ 16 + 36 + 66 -328 +554
+	10.40	- 36.66	+ 8 + 83 + 65 +648 +196
+	14.65	- 32.41	- 12 -248 +719 + 0 - 21

32S(1,0)

	4	- 47.06	s3d1 s2d2 s1d3 s1d3 1131 1010 1111 1131
+	7.54	- 39.52	-591 - 23 + 32 -355
+	10.82	- 36.24	+ 18 -859 + 98 + 25
+	11.49	- 35.57	-364 - 11 -154 +472
+	15.38	- 31.68	- 28 +107 +716 +149

32S(4,0)

	3	- 47.06	s2d2 s1d3 d4 1030 1171 40
+	5.95	- 41.11	-822 +171 - 7
+	9.55	- 37.51	+166 +652 -182
+	12.11	- 34.95	+ 12 +177 +811

32S(3,0)

	3	- 47.06	s2d2 s1d3 s1d3 1030 1151 1171
+	8.18	- 38.88	- 69 -446 +484
+	9.56	- 37.50	+920 - 67 + 13
+	14.00	- 33.06	+ 11 +487 +503

33Cl/S(1/2,1/2)

	8	- 55.71	s3d2 s3d2 s2d3 s2d3 s2d3 s1d4 s1d4 d5 1110 1101 0111 1031 1011 1100 1111 11
+	1.03	- 54.68	-112 +732 + 13 + 3 + 15 -125 - 0 + 0
+	3.83	- 51.88	+ 88 - 16 -146 - 5 - 70 -644 - 18 + 13
+	6.19	- 49.52	+ 86 - 10 +192 +547 + 44 - 36 - 78 - 9
+	7.95	- 47.76	-526 -229 + 93 - 0 + 1 -136 + 15 - 0
+	9.24	- 46.46	- 83 + 2 -172 +413 -236 + 30 + 40 + 24
+	11.83	- 43.87	+ 47 - 0 + 11 + 5 + 96 - 10 +453 +378
+	12.40	- 43.30	- 49 - 4 - 50 + 0 +102 + 15 -371 +408
+	14.44	- 41.27	- 8 - 7 -324 + 27 +436 - 4 + 25 -168

33Cl/S(7/2,1/2)

	7	- 55.71	s3d2 s2d3 s2d3 s2d3 s1d4 s1d4 d5 1130 0171 1051 1071 1140 1131 71
+	2.77	- 52.94	-801 +100 - 8 - 17 + 0 - 67 - 7
+	4.67	- 51.04	+ 36 +432 -350 + 35 - 29 + 95 - 23
+	7.46	- 48.24	+126 +109 + 17 + 1 + 31 -590 -126
+	8.55	- 47.16	+ 11 - 50 -449 -222 + 89 - 68 +110
+	9.02	- 46.68	- 12 - 2 - 18 +641 +137 - 28 +162
+	10.70	- 45.01	+ 14 +273 +130 - 58 - 1 - 0 +524
+	12.91	- 42.80	- 0 + 35 + 28 - 26 +712 +151 - 47

33Cl/S(5/2,1/2)

	11	- 55.71	s3d2 s3d2 s2d3 s2d3 s2d3 s2d3 s1d4 s1d4 s1d4 s1d4 d5 1130 1121 0151 1031 1051 1071 1120 1120"1121 1131 51
+	1.38	- 54.32	+ 81 -665 - 1 + 19 - 6 - 0 - 74 - 16 -118 + 15 + 5
+	3.74	- 51.97	- 13 + 1 -142 +670 - 7 - 16 +132 - 13 - 1 + 1 + 4
+	5.64	- 50.06	-474 + 17 - 23 - 1 - 13 - 32 -252 - 7 -155 - 0 + 27
+	6.38	- 49.33	-192 -243 - 2 - 1 + 13 - 23 + 1 + 5 +266 -207 - 47
+	6.81	- 48.90	- 16 + 4 +479 +240 + 41 +114 - 53 + 0 - 4 - 10 - 39
+	7.70	- 48.01	-130 - 38 + 93 - 52 - 50 + 15 +453 - 10 -151 + 5 - 3
+	10.36	- 45.35	+ 15 + 9 + 0 + 2 -733 + 4 - 27 - 6 + 8 - 39 -157
+	11.11	- 44.60	+ 53 + 19 - 0 - 2 + 81 -200 + 4 - 28 -202 -215 -197
+	11.47	- 44.23	+ 7 + 4 + 0 - 4 - 0 + 69 + 0 -498 + 7 -205 +206
+	12.28	- 43.43	- 15 + 0 - 10 - 5 + 30 + 2 - 4 -387 + 37 +268 -242
+	13.40	- 42.30	+ 3 + 0 +250 + 3 - 26 -526 + 0 - 31 + 52 + 35 + 74

33Cl/S(9/2,1/2)

	?	- 55.71	s2d3 s1d4 1071 1140
+	5.34	- 50.37	-920 - 80
+	8.57	- 47.13	- 80 +920

For the meaning of the symbols used see subsect. 2.3.

TABLE 2 (continued)

33C1/S(3/2,1/2)

			s4d1	s3d2	s3d2	s2d3	s2d3	s2d3	s2d3	s2d3	s1d4	s1d4	s1d4	s1d4	d5
	13	- 55.71	0021	1110	1121	0131	0133	1011	1031	1051	1120	1120"	1121	1111	31
-	.08	- 55.78	-621	- 6	+ 16	-160	-127	+ 18	+ 0	- 20	+ 10	- 1	- 0	- 0	+ 20
+	2.77	- 52.94	+ 10	+183	- 75	-354	+ 89	- 3	+242	- 0	+ 13	- 5	- 10	- 16	- 1
+	3.65	- 52.05	-261	- 9	+ 2	+ 27	+341	- 64	+ 13	+ 77	- 36	- 2	+ 32	+ 13	-122
+	4.97	- 50.74	+ 76	-359	+140	-133	+ 31	+ 3	+ 45	+ 0	+ 29	- 12	+ 82	+ 72	+ 17
+	6.37	- 49.34	+ 2	+ 77	- 20	- 19	- 26	+ 2	- 5	+ 2	-326	- 20	+380	+ 76	+ 45
+	7.22	- 48.48	+ 10	- 85	- 15	- 28	- 34	+114	+ 7	- 26	-168	- 13	- 8	- 32	-460
+	7.94	- 47.76	-	4	- 19	- 2	+180	- 39	+ 7	+633	+ 0	- 34	+ 5	- 1	- 6	+ 70
+	8.48	- 47.23	-	4	-185	-393	- 18	+ 46	+ 3	- 30	+ 3	- 49	+ 28	- 93	+ 22	+128
+	10.28	- 45.43	-	2	+ 0	-149	+ 29	- 24	- 10	+ 16	-128	+145	- 17	+ 8	+397	- 76
+	10.99	- 44.71	+	3	- 11	+ 19	- 11	- 8	-593	+ 0	-222	- 98	- 1	- 25	- 5	+ 2
+	12.55	- 43.16	-	0	- 53	-130	+ 7	- 8	- 38	- 4	+ 10	+ 65	-313	+108	-258	+ 5
+	14.50	- 41.21	+	5	- 11	- 19	- 35	-193	-139	+	4	+319	+ 10	+200	+ 12	+ 1	- 51
+	14.85	- 40.86	-	1	- 4	- 19	+ 1	+ 36	+ 5	-	0	-193	+ 17	+381	+241	-100	- 1

33P(3/2,3/2)

			s3d2	s2d3	s2d3	s2d3	s1d4	s1d4	d5
	7	- 50.08	1121	0131	0133	1033	1111	1121	33
+	1.37	- 48.71	+155	+597	-109	- 75	- 0	- 7	+ 57
+	3.00	- 47.08	-339	+328	+286	+ 26	+ 18	+ 1	+ 2
+	3.48	- 46.60	-452	- 2	-297	-128	- 43	+ 48	+ 29
+	6.36	- 43.72	+ 49	+ 0	+122	- 19	-250	+537	+ 23
+	6.71	- 43.37	+ 0	- 2	- 41	+497	- 8	+ 1	+451
+	8.16	- 41.92	+ 0	+ 49	-143	+200	+ 35	+252	-320
+	9.16	- 40.92	-	4	+ 22	- 2	+ 55	-645	-154	-117

33P(1/2,3/2)

			s3d2	s2d3	s2d3	s1d4	s1d4
	5	- 50.08	1101	0111	1033	1111	1102
-	.02	- 50.09	-879	- 16	+ 0	+ 10	+ 94
+	4.61	- 45.47	- 41	+388	-436	- 83	- 52
+	4.75	- 45.32	- 64	- 85	+ 69	-202	-580
+	9.96	- 40.12	+ 9	-511	-465	- 11	+ 5
+	11.07	- 39.00	-	7	- 0	- 30	+694	-269

33P(5/2,3/2)

			s3d2	s2d3	s2d3	s1d4	s1d4
	5	- 50.08	1121	0131	1033	1121	1131
+	2.50	- 47.57	-743	+ 17	+201	+ 39	+ 1
+	3.08	- 46.99	- 94	-337	-377	+172	+ 19
+	5.28	- 44.80	-158	+ 4	-187	-570	- 81
+	7.22	- 42.86	+ 1	-530	+196	-190	+ 83
+	8.63	- 41.45	- 4	+113	- 39	- 28	+816

33P(7/2,3/2)

			s2d3	s1d4
	2	- 50.08	0111	1131
+	4.44	- 45.64	-822	+178
+	5.84	- 44.23	+178	+822

34C1(3,0)

			s4d2	s3d3	s3d3	s2d4	s2d4	s2d4	s2d4	s1d5	s1d5	d6
	10	- 67.16	0030	1151	1171	0131	1020	1020"	1040	1151	1171	30
+	.02	- 67.13	-780	+ 23	+ 81	+101	+ 0	- 0	- 2	+ 1	+ 6	+ 6
+	1.86	- 65.29	+ 31	+595	+159	- 77	+ 11	- 8	+ 10	+ 87	+ 22	- 2
+	3.97	- 63.18	- 0	- 0	+ 4	- 4	-950	- 0	+ 1	+ 35	+ 5	- 0
+	5.03	- 62.13	-150	- 3	- 23	-494	+ 0	+ 0	+ 48	- 9	- 64	-209
+	6.69	- 60.46	- 16	-106	- 47	- 40	+ 32	- 6	+ 18	+475	+224	+ 37
+	7.82	- 59.33	+ 9	-149	+441	- 27	+ 1	+118	+122	- 60	+ 67	+ 7
+	9.41	- 57.74	+ 12	- 66	+102	+ 69	+ 3	-165	- 19	+ 40	+ 4	-521
+	9.60	- 57.56	-	0	- 8	+ 10	- 20	- 0	-700	+ 50	- 71	- 2	+138
+	12.95	- 54.21	-	0	- 49	+133	- 70	+ 2	+ 0	-298	+ 96	-274	+ 78
+	14.10	- 53.06	+	2	- 1	+ 1	+ 98	+ 1	+ 3	+432	+127	-334	+ 1

34C1/S(0,1)

			s4d2	s3d3	s2d4	s2d4	s2d4	s1d5	d5
	7	- 67.16	0001	1111	0100	0102	1011	1111	01
+	.04	- 67.12	-709	- 9	+124	-115	- 27	- 0	+ 16
+	3.82	- 63.33	-169	- 70	+674	- 8	+ 21	+ 4	- 54
+	5.16	- 62.00	- 81	+ 8	+112	+529	+167	- 19	- 93
+	8.87	- 58.29	+ 15	-762	+ 29	+ 49	+ 1	+ 34	+109
+	9.28	- 57.88	+ 17	-128	+ 32	- 29	-103	- 68	-624
+	12.69	- 54.47	- 1	+ 16	+ 9	+ 16	- 52	+831	- 76
+	16.46	- 50.70	- 8	+ 7	- 20	+255	-629	- 43	+ 39

34C1(1,0)

			s4d2	s3d3	s3d3	s2d4	s2d4	s2d4	s2d4	s1d5	s1d5	d6
	10	- 67.16	0010	1111	1131	0111	1000	1020	1020"	1111	1151	10
+	.22	- 66.94	- 85	+ 41	+792	- 25	+ 3	+ 20	- 5	+ 0	+ 29	+ 0
+	1.47	- 65.68	-389	+167	- 29	- 75	+305	- 1	- 0	- 17	- 10	+ 7
+	2.98	- 64.18	+383	- 0	+ 17	+ 1	+554	+ 2	- 0	- 24	+ 19	+ 0
+	3.81	- 63.34	- 8	-133	- 3	+ 73	- 23	+ 36	+ 10	- 89	+611	- 14
+	6.51	- 60.64	+ 38	-504	+124	+ 59	- 36	- 0	- 38	- 18	-181	+ 0
+	7.89	- 59.27	+ 56	- 7	- 3	+379	- 62	+ 51	+ 0	- 96	+ 4	+343
+	7.96	- 59.20	+ 0	+ 2	+ 11	- 1	- 3	-854	+ 0	- 84	+ 27	+ 18
+	9.94	- 57.21	- 38	+137	- 3	+230	+ 2	+ 33	- 10	-414	- 60	+ 72
+	12.24	- 54.91	- 3	- 8	+ 4	+154	+ 9	- 2	+ 80	+217	+ 10	+513
+	13.47	- 53.68	+ 1	- 1	+ 15	- 2	- 1	+ 0	+857	- 42	- 48	- 33

34C1(2,0)

			s3d3	s3d3	s2d4	s2d4	s2d4	s1d5	s1d5
	7	- 67.16	1131	1151	0121	1020	1020"	1131	1151
+	1.49	- 65.66	+427	+ 61	+180	+299	+ 6	+ 62	- 5
+	2.53	- 64.62	+420	+ 3	-408	- 81	- 76	+ 1	+ 11
+	5.97	- 61.19	+ 15	+181	+ 57	- 15	- 3	-645	+ 83
+	8.25	- 58.90	+ 3	-331	- 28	+352	- 80	-199	- 7
+	8.61	- 58.55	-127	+308	-150	+258	- 58	+ 26	+ 72
+	12.35	- 54.80	+ 7	- 59	- 24	+ 17	+410	+ 0	+483
+	13.71	- 53.44	+ 0	+ 58	-152	+ 17	+367	- 67	-338

34C1/S(4,1)

			s3d3	s2d4	s2d4	s1d5
	4	- 67.16	1171	0140	1031	1171
+	5.47	- 61.69	-881	- 18	- 66	+ 35
+	6.87	- 60.28	- 27	-252	+720	- 1
+	9.15	- 58.01	+ 81	-238	- 44	+637
+	10.91	- 56.24	+ 10	-492	-170	-328

34C1(4,0)

			s3d3	s2d4	s1d5
	3	- 67.16	1171	1040	1171
+	2.05	- 65.10	-831	+ 40	-130
+	7.05	- 60.10	-163	+ 68	+770
+	9.51	- 57.64	+ 7	-893	+101

34C1(0,0)

			s3d3	s1d5
	2	- 67.16	1111	1111
+	11.77	- 55.38	-876	-124
+	16.75	- 50.41	-124	+876

For the meaning of the symbols used see subsect. 2.3.

TABLE 2 (continued)

34Cl/S(1,1)

9	− 67.16	a3d3 a3d3 a3d3 a2d4 a2d4 a2d4 a1d5 a1d5 a1d5
		1111 1131 1133 0111 1011 1021 1111 1131 1133
+ 4.97	− 62.19	+ 97 −615 −208 + 2 + 2 − 0 + 1 + 53 + 20
+ 6.82	− 60.34	−194 −214 +325 +139 − 0 − 81 + 6 − 5 + 37
+ 7.99	− 59.17	+ 21 + 62 − 58 +418 + 0 −296 − 26 + 41 − 77
+ 9.11	− 58.04	− 68 + 51 − 5 − 0 − 36 + 2 +114 +993 +131
+ 11.39	− 55.76	−484 − 23 − 88 − 5 + 16 + 35 − 97 + 26 −225
+ 12.35	− 54.82	− 1 + 11 − 0 + 0 +930 − 2 + 28 + 3 + 25
+ 12.69	− 54.47	+121 − 5 +281 + 0 + 15 + 70 −215 +251 − 43
+ 13.55	− 53.61	− 0 − 4 + 8 −434 + 0 −512 − 12 + 22 − 9
+ 15.92	− 51.23	+ 14 − 14 + 27 − 0 − 0 + 2 +502 + 7 −433

34Cl/S(3,1)

7	− 67.16	a3d3 a3d3 a2d4 a2d4 a2d4 a1d5 a1d5
		1151 1171 1031 1021 1031 1151 1171
+ 5.32	− 61.84	−279 + 51 +263 −390 − 3 − 13 + 1
+ 7.27	− 59.88	+380 −232 + 58 −204 + 29 − 83 + 13
+ 8.58	− 58.58	+187 +580 + 86 + 25 + 85 − 36 − 1
+ 9.77	− 57.39	+ 7 + 74 −474 −331 + 28 + 1 − 84
+ 10.55	− 56.63	−140 − 24 − 19 + 25 +625 −137 + 29
+ 11.30	− 55.85	− 1 + 25 − 95 + 0 −200 −411 +269
+ 12.98	− 54.17	− 6 − 13 + 5 + 24 − 30 −319 −604

34Cl/S(2,1)

14	− 67.16	a4d2 a3d3 a3d3 a3d3 a2d4 a2d4 a2d4 a2d4 a2d4 a2d4 a1d5 a1d5 a1d5 d6
		0021 1131 1151 1133 0120 0120*0121 1011 1021 1031 1131 1151 1133 21
+ 2.17	− 64.98	−352 +323 + 2 −175 − 7 − 13 − 53 − 1 + 4 − 4 + 24 − 0 − 41 + 3
+ 3.21	− 63.94	−245 −470 + 7 − 10 −176 − 0 − 15 − 0 + 4 − 0 + 23 + 7 + 39 − 1
+ 3.44	− 63.71	−107 + 18 −142 +473 + 2 − 2 −130 − 32 + 0 − 7 − 53 + 8 + 23 + 2
+ 5.73	− 61.42	+ 7 − 65 − 6 − 61 +326 + 8 −240 − 27 −104 − 25 + 65 + 3 + 2 + 62
+ 6.25	− 60.90	−238 − 19 + 8 − 2 +223 + 16 +114 + 52 − 67 + 20 −211 − 29 − 1 − 2
+ 7.85	− 59.30	+ 15 + 14 + 97 − 85 + 0 + 1 − 49 − 30 + 44 − 3 −288 + 50 +318 − 5
+ 8.98	− 58.57	+ 13 − 30 + 24 − 0 − 44 + 37 −138 − 0 + 10 − 17 −219 − 72 −364 + 30
+ 9.35	− 57.61	+ 0 + 35 + 31 + 4 −108 +219 − 0 − 76 −457 + 2 + 2 − 8 + 9 − 48
+ 9.84	− 57.31	+ 10 − 0 −439 −108 − 42 + 12 − 2 +183 − 38 − 60 − 47 + 30 + 2 − 25
+ 11.52	− 55.64	− 0 + 18 + 88 + 36 − 17 + 31 − 2 +317 − 16 − 0 + 4 + 80 + 17 +374
+ 12.38	− 54.78	− 0 + 0 +144 + 45 + 23 − 11 − 27 +117 − 1 −277 + 14 + 9 − 9 −323
+ 13.19	− 53.96	− 8 + 2 − 9 + 0 + 27 +645 + 4 + 0 +249 − 9 + 38 − 0 + 1 − 8
+ 13.81	− 53.34	− 5 − 1 + 0 − 0 − 2 − 1 +224 −135 − 3 −503 − 6 + 22 − 3 + 97
+ 14.51	− 52.65	+ 0 + 4 − 1 − 0 − 4 − 4 − 2 + 28 + 1 − 74 + 6 −682 +172 + 20

34Cl(5,0)

1	− 67.16	a2d4
		1040
+ 5.43	− 61.73	+1000

34P(1,2)

4	− 56.65	a3d3 a2d4 a2d4 a1d5
		1133 0111 1002 1133
+ .35	− 56.30	−873 − 81 − 20 + 26
+ 1.55	− 55.10	− 85 +298 +616 − 1
+ 4.24	− 52.41	+ 34 − 43 + 65 +858
+ 6.24	− 50.41	+ 8 −578 +299 −115

34P(2,2)

3	− 56.65	a3d3 a2d4 a1d5
		1133 0121 1122
+ .45	− 56.20	−975 + 5 + 19
+ 1.85	− 54.80	− 4 −991 + 4
+ 4.36	− 52.29	+ 20 + 3 +976

34P(0,2)

1	− 56.65	a2d4
		0102
+ 1.89	− 54.76	+1000

34P(3,2)

1	− 57.65	a2d4
		0131
+ 3.55	− 54.10	+1000

35Cl/Ar(1/2,1/2)

8	− 79.85	a4d3 a3d4 a3d4 a2d5 a2d5 a2d5 a1d6 a1d6
		0011 1100 1111 0111 1011 1021 1111 1101
+ 1.26	− 78.59	+ 23 −895 + 16 + 12 − 4 − 0 + 0 + 49
+ 5.20	− 74.65	−460 − 3 + 22 −193 + 65 − 60 + 31 +165
+ 6.37	− 73.48	+312 + 25 −100 − 28 + 49 + 0 +123 +363
+ 7.61	− 72.24	−179 − 4 −241 + 71 − 27 +413 + 38 + 26
+ 9.68	− 70.17	− 3 − 37 −540 − 41 − 10 −247 + 6 −115
+ 10.96	− 69.29	+ 15 − 35 − 0 −309 +207 +248 + 3 −183
+ 13.34	− 66.51	+ 1 + 0 + 80 − 6 −164 − 0 +688 − 60
+ 15.62	− 64.23	+ 7 + 1 − 0 −339 −473 + 30 −111 + 38

35Cl/Ar(7/2,1/2)

7	− 79.85	a4d3 a3d4 a3d4 a2d5 a2d5 a2d5 a1d6
		0071 1140 1131 0171 1051 1071 1130
+ 2.82	− 77.04	−830 − 10 + 55 − 88 − 4 − 0 + 13
+ 4.11	− 75.74	+ 21 +113 +718 + 24 + 55 − 18 + 51
+ 6.33	− 73.52	−113 + 1 − 15 +437 +283 + 0 −150
+ 8.51	− 71.34	+ 3 −289 − 20 + 7 +145 −171 +366
+ 9.84	− 70.02	− 29 +262 − 77 +127 −185 −234 + 88
+ 10.28	− 69.57	− 4 +179 − 78 − 6 +113 +351 +270
+ 11.95	− 67.91	− 1 −146 + 37 +312 −215 +226 + 63

35Cl/Ar(5/2,1/2)

11	− 79.85	a4d3 a3d4 a3d4 a3d4 a3d4 a2d5 a2d5 a2d5 a2d5 a1d6 a1d6
		0051 1120 1120*1121 1131 0151 1051 1051 1071 1130 1121
+ 1.67	− 78.18	+137 +333 + 6 −378 − 63 + 0 + 1 − 4 − 0 − 6 − 73
+ 3.55	− 76.30	−265 +362 + 8 + 36 + 55 − 87 +172 + 9 + 4 + 0 − 2
+ 5.12	− 74.73	−455 − 83 + 29 −294 − 19 − 28 − 74 − 6 + 3 − 7 − 41
+ 5.81	− 74.04	+ 23 −144 + 80 − 48 − 46 − 62 +527 + 0 + 14 − 1 + 56
+ 8.01	− 71.84	+ 4 − 0 +105 −130 +418 + 12 − 4 − 0 − 46 +208 + 73
+ 8.38	− 71.47	+ 1 + 40 − 1 − 2 − 77 −160 −141 + 24 + 72 + 26 +456
+ 8.62	− 71.23	+104 − 25 + 5 + 1 +169 −340 − 33 + 49 +106 − 23 −145
+ 9.56	− 70.29	− 1 − 6 −704 − 83 + 42 − 29 + 36 − 70 + 5 + 22 + 2
+ 11.82	− 68.03	− 4 − 4 − 60 − 41 − 0 + 12 + 6 +800 − 66 − 6 + 0
+ 12.39	− 67.46	+ 0 − 3 − 0 + 24 −110 − 44 + 0 + 7 − 21 +646 −145
+ 14.44	− 65.41	+ 5 − 0 − 0 + 4 − 1 −226 − 6 − 30 −664 − 57 + 7

35Cl/Ar(9/2,1/2)

2	− 79.85	a3d4 a2d5
		1140 1071
+ 5.35	− 74.50	−751 −249
+ 7.38	− 72.47	−249 +751

For the meaning of the symbols used see subsect. 2.3.

TABLE 2 (continued)

35Cl/Ar(3/2,1/2)

			a4d3	a3d4	a3d4	a3d4	a3d4	a2d5	a2d5	a2d5	a2d5	a1d6	a1d6	d7
	13	- 79.85	0031	1120	1120"	1121	1111	0131	0133	1011	1031	1051	1110	1121	31
+ .06		- 79.79	-790	- 38	+ 3	+ 1	- 2	- 46	- 95	+ 8	+ 0	- 10	+ 0	+ 2	+ 7
+ 2.65		- 77.20	+ 48	-197	- 47	-289	+120	-192	- 9	+ 8	- 43	- 26	- 8	- 2	+ 10
+ 4.70		- 75.15	- 2	- 2	- 1	+127	- 62	-290	+248	- 15	-229	+ 17	- 5	- 1	+ 0
+ 5.15		- 74.70	- 80	-156	+ 1	-105	+ 4	+189	+243	- 79	- 4	+ 40	- 5	- 6	- 88
+ 6.07		- 73.78	- 54	+482	- 4	- 45	+197	- 1	+ 4	- 0	- 64	+ 3	- 67	- 71	- 8
+ 8.75		- 71.10	+ 6	- 71	+169	+222	+356	+ 21	- 19	+ 4	- 57	+ 10	- 42	+ 23	- 0
+ 9.47		- 70.38	+ 1	+ 0	- 11	- 6	- 64	+141	- 75	+ 34	-577	- 21	+ 55	+ 2	- 14
+ 10.17		- 69.68	+ 8	- 14	+ 2	+ 12	- 67	- 5	- 45	+ 6	+ 5	- 57	-301	-125	-350
+ 11.00		- 68.85	- 1	+ 1	- 0	+ 1	+ 41	- 42	+ 28	+252	+ 14	+ 11	+234	+ 11	-364
+ 11.66		- 68.19	+ 3	+ 2	+645	-110	- 43	- 5	+ 11	+ 74	- 2	+ 1	+ 3	- 66	+ 35
+ 12.67		- 67.18	+ 1	+ 14	+100	- 3	+ 9	- 25	- 1	-368	- 1	-290	+ 83	+ 36	- 69
+ 15.29		- 64.56	+ 1	+ 19	+ 17	- 79	- 34	- 18	- 29	- 3	- 2	+152	-108	+501	- 38
+ 15.97		- 63.88	+ 6	- 5	+ 1	+ 0	- 0	- 24	-193	-149	- 2	+362	+ 88	-153	- 18

35S(3/2,3/2)

			a4d3	a3d4	a3d4	a2d5	a2d5	a2d5	a1d6
	7	- 74.10	0033	1111	1121	0131	0133	1033	1121
- .09		- 74.19	-813	+ 13	+ 1	+121	- 41	+ 10	+ 1
+ 3.04		- 71.06	+ 17	-234	-362	+355	+ 15	- 1	+ 16
+ 4.10		- 70.01	-155	- 83	- 56	-232	+233	-229	- 13
+ 5.58		- 69.52	- 2	+ 1	-363	-231	-350	+ 24	+ 29
+ 6.54		- 67.57	+ 2	+649	-177	+ 14	+144	- 6	+ 8
+ 8.19		- 65.91	- 1	- 0	- 41	- 1	+ 12	+222	-724
+ 8.78		- 65.32	- 11	- 20	+ 1	- 46	+205	+509	+208

35S(7/2,3/2)

			a3d4	a2d5
	2	- 74.10	1131	0171
+ 2.92		- 71.18	-968	+ 32
+ 5.95		- 68.16	+ 32	+968

35S(1/2,3/2)

			a3d4	a3d4	a2d5	a2d5	a1d6
	5	- 74.10	1111	1102	0111	1033	1101
+ 1.18		- 72.93	-207	+681	+ 5	- 1	-107
+ 5.47		- 68.64	- 35	+ 49	-297	+178	+442
+ 5.80		- 68.30	-188	- 4	+170	-299	+339
+ 8.82		- 65.28	-569	-267	- 31	+ 38	- 95
+ 11.18		- 62.93	- 1	- 0	+497	+485	+ 17

35S(5/2,3/2)

			a3d4	a3d4	a2d5	a2d5	a1d6
	5	- 74.10	1121	1131	0151	1033	1121
+ 2.07		- 72.04	-836	+ 80	- 61	- 10	+ 13
+ 4.38		- 69.72	- 43	- 1	+252	+690	+ 35
+ 5.71		- 68.39	+ 85	+871	- 11	+ 31	- 2
+ 7.82		- 66.29	- 36	+ 13	+284	- 29	-638
+ 8.82		- 65.29	+ 0	+ 35	+413	-240	+311

36Ar(2,0)

			a4d4	a4d4	a3d5	a3d5	a2d6	a2d6	a2d6	a1d7
	8	- 95.10	0020	0020"	1131	1151	0121	1010	1030	1131
+ 2.23		- 92.87	-551	- 14	+347	+ 31	- 23	+ 0	- 2	+ 31
+ 4.20		- 90.90	-340	+ 34	-465	- 17	- 85	+ 20	- 2	- 36
+ 7.88		- 87.23	- 77	+ 0	- 1	+ 4	+425	-201	+ 77	-215
+ 8.94		- 86.17	+ 1	-839	- 30	+ 45	- 10	+ 11	- 1	- 63
+ 10.50		- 84.60	+ 14	+108	+ 1	+676	- 16	+ 29	- 15	-142
+ 11.33		- 83.78	+ 8	+ 4	+142	-211	- 97	+ 0	- 36	-503
+ 13.04		- 82.06	- 1	+ 1	+ 13	- 10	+ 46	+594	+324	- 10
+ 15.82		- 79.29	- 8	- 0	- 0	- 7	+298	+144	-542	+ 0

36Ar(0,0)

			a4d4	a3d5	a2d6	a2d6	d8
	5	- 95.10	0000	1111	0101	1010	00
+ .21		- 94.90	-856	+ 8	-120	- 10	- 6
+ 4.20		- 90.90	+ 62	-329	-433	-130	- 46
+ 8.77		- 86.34	- 73	-639	+161	+ 26	+101
+ 12.52		- 82.58	+ 3	+ 25	- 33	-165	+776
+ 17.10		- 78.01	+ 6	- 0	-252	+670	+ 72

36Ar(1,0)

			a3d5	a3d5	a2d6	a1d7
	4	- 95.10	1111	1131	1010	1131
+ 8.02		- 87.08	+117	+810	+ 6	+ 68
+ 12.06		- 83.04	+479	- 87	+429	- 6
+ 14.32		- 80.79	-325	+ 1	+448	+226
+ 16.34		- 78.76	- 80	+103	+118	-700

36Ar(4,0)

			a4d4	a3d5	a2d6
	3	- 95.10	0040	1171	1030
+ 5.69		- 89.42	-637	+299	+ 64
+ 7.55		- 87.56	+331	+321	+349
+ 10.10		- 85.00	- 32	-381	+587

36Ar(3,0)

			a3d5	a3d5	a2d6
	3	- 95.10	1151	1171	1030
+ 6.83		- 88.27	-494	+501	+ 5
+ 11.62		- 83.49	+133	+ 75	+792
+ 12.78		- 82.33	+373	+424	-203

36Cl(1,1)

			a4d4	a3d5	a3d5	a3d5	a2d6	a2d6	a2d6	a1d7
	8	- 88.43	0011	1111	1131	1133	0110	1001	1021	1131
+ 1.16		- 87.28	- 69	-148	-136	+600	- 12	- 8	+ 11	- 16
+ 1.61		- 86.82	-360	- 23	+555	+ 11	+ 38	+ 0	- 8	- 6
+ 2.96		- 85.47	-264	+101	-193	- 6	+138	+269	- 6	+ 22
+ 4.37		- 84.06	-265	+ 3	- 67	-138	- 54	-455	+ 5	+ 14
+ 6.71		- 81.73	+ 22	-174	- 5	+ 0	+216	- 50	-193	+340
+ 7.41		- 81.02	- 14	-270	+ 1	- 73	-225	+200	+ 60	+158
+ 8.80		- 79.63	+ 1	+252	+ 44	+160	- 25	- 7	+ 68	+444
+ 10.79		- 77.64	-	5	+ 30	+ 0	+ 12	-293	+ 12	-649	+ 0

36Cl(2,1)

			a4d4	a3d5	a3d5	a3d5	a2d6	a2d6	a2d6	a1d7
	7	- 88.43	0021	1131	1151	1133	0121	1021	1131
- .17		- 88.60	-864	- 28	- 20	+ 5	- 75	+ 8	+ 0	
+ 1.22		- 87.22	- 11	+673	- 66	+206	+ 8	+ 0	- 36	
+ 3.24		- 85.20	+ 49	-255	- 95	+530	- 1	+ 49	- 24	
+ 4.89		- 83.54	- 52	- 38	- 4	+ 9	+604	-292	- 1	
+ 7.11		- 81.32	- 12	- 2	+271	- 0	+ 21	+ 62	-633	
+ 8.77		- 79.66	+ 6	- 4	-535	-234	+ 0	+ 1	-220	
+ 10.02		- 78.41	- 7	+ 1	- 7	- 15	+291	+593	+ 86	

For the meaning of the symbols used see subsect. 2.3.

TABLE 2 (continued)

36Cl(3,1)

	5	- 88.43	s4d4	s3d5	s3d5	s2d6	s2d6
			0031	1151	1171	0130	1021
+	.72	- 87.71	-898	- 24	+ 13	- 61	- 3
+	3.84	- 84.59	-	0	-665	+219	+113 + 2
+	4.60	- 83.83	-	65	+ 95	- 1	+376 +464
+	6.40	- 82.03	-	36	+199	-380	+ 80 -306
+	7.46	- 80.97	-	1	- 17	+387	+370 -225

36Cl(0,1)

	2	- 88.43	s3d5	s2d6	
			1111	0101	
+	3.30	- 85.13	+ 47	+953	
+	9.26	- 79.17	-953	+ 47	

36Cl(4,1)

	1	- 88.43	s3d5		
			1171		
+	2.88	- 85.55	+1000		

36S(0,2)

	2	- 83.99	s4d4	s2d6
			0002	0101
-	.00	- 83.99	-858	+142
+	4.28	- 79.71	+142	+858

36S(2,2)

	2	- 83.99	s3d5	s2d6	
			1133	0121	
+	2.83	- 81.16	-965	- 35	
+	6.23	- 77.76	- 35	+965	

36S(1,2)

	1	- 83.99	s3d5	
			1133	
+	5.75	- 78.24	+1000	

37Ar/K(3/2,1/2)

	5	-103.90	s4d5	s3d6	s3d6	s2d7	s2d7
			0021	1110	1121	0131	1031
-	.25	-104.13	-915	+ 9	- 20	- 55	+ 3
+	3.21	-100.69	+	6	+278	-583	+100 - 34
+	5.78	- 98.12	+	68	+ 4	-127	-505 +296
+	7.87	- 96.02	+	1	+709	+270	- 11 + 8
+	10.21	- 93.69	+	10	+ 1	- 0	-330 -659

37Ar/K(1/2,1/2)

	5	-103.90	s4d5	s3d6	s3d6	s2d7	s1d8	
			0011	1101	1110	1031	1100	
+	1.32	-102.58	-113	+702	-133	+ 3	+ 49	
+	5.47	- 98.42	+822	+116	+ 8	+ 1	+ 53	
+	7.98	- 95.91	-	61	+ 7	+557	- 41	+353
+	9.07	- 94.83	-	0	-140	-124	+264	+471
+	10.09	- 93.81	-	3	+ 34	+178	+691	- 93

37Ar/K(5/2,1/2)

	4	-103.90	s4d5	s3d6	s3d6	s2d7
			0051	1130	1121	1021
+	3.75	-100.14	-969	- 4	+ 24	+ 4
+	4.62	- 99.27	+ 29	-357	+500	+114
+	6.92	- 96.98	+	0	+245	- 0 +754
+	8.18	- 95.71	+	2	+394	+476 -128

37Ar/K(7/2,1/2)

	2	-103.90	s4d5	s3d6
			0071	1130
+	2.12	-101.77	-809	-191
+	4.50	- 99.40	-191	+809

37Cl(3/2,3/2)

	3	- 98.75	s4d5	s3d6	s2d7
			0033	1121	0131
+	.07	- 98.68	-928	- 20	+ 52
+	4.94	- 93.81	-	71	+155 -774
+	6.37	- 92.38	-	1	+825 +173

37Cl(1/2,3/2)

	1	- 98.75	s3d6	
			1101	
+	1.49	- 97.26	+1000	

37Cl(5/2,3/2)

	1	- 98.75	s3d6	
			1121	
+	2.53	- 96.23	+1000	

38K(1,0)

	3	-115.93	s4d6	s3d7	s2d8
			0010	1131	1000
+	.77	-115.17	+355	+643	- 2
+	2.26	-113.67	-644	+351	- 5
+	5.31	-110.63	-	1	+ 6 +293

38K(3,0)

	1	-115.93	s4d6	
			0030	
+	.01	-115.93	+1000	

38K(2,0)

	1	-115.93	s3d7	
			1131	
+	3.92	-112.01	+1000	

38Ar/K(0,1)

	2	-115.74	s4d6	s2d8	
			0001	0100	
-	.17	-115.91	-947	- 53	
+	6.50	-109.24	-	53	+947

38Ar/K(2,1)

	2	-115.74	s4d6	s3d7	
			0021	1131	
+	2.37	-113.37	-868	-132	
+	4.21	-111.53	-132	+868	

38Ar/K(1,1)

	1	-115.74	s3d7	
			1131	
+	7.77	-108.97	+1000	

39K/Ca(3/2,1/2)

	1	-129.02	s4d7	
			0031	
+	.04	-128.98	+1000	

39K/Ca(1/2,1/2)

	1	-129.02	s3d8	
			1100	
+	2.56	-126.46	+1000	

40Ca(0,0)

	1	-144.04	s4d8	
			0000	
-	.04	-144.07	+1000	

For the meaning of the symbols used see subsect. 2.3.

mirror nuclei where the average value is given), and the pure configurations that can couple to the particular pair of (J, T) values. The configurations are given as, e.g.,

$$\underset{j_1\ t_1\ \underline{j_2}\ \underline{t_2}}{\mathrm{s\ n\ d\ m}} \equiv \mathrm{s}^n_{j_1 t_1}\,\mathrm{d}^m_{\underline{j_2}\,\underline{t_2}},$$

where the underlining indicates half integer spins; the double prime at the configuration $^{d4}_{20''}$ indicates the seniority $v = 4$; the unprimed configuration $^{d4}_{20}$ denotes the $v = 2$ case. Intensities of the various pure wave functions (as indicated at the top of each column), constituting the mixed configuration of a particular state, are given in tenths of a percent and thus add up to 1000. The sign which is given refers to the amplitude.

The two columns of numbers that label the rows of the table of intensities, give the excitation energy (the computed energy relative to the experimental ground-state energy) in the first column, and the computed energy in the second column.

The computed and the experimental level energies are shown in figs. 2 through 5 (all excitations above 5 MeV were left out). Large level densities are denoted by hatched areas. The states that have been used to obtain the values of the parameters are represented by bold lines. The experimental level energies were taken from ref. [4]).

^{29}Si/P *nuclei.* For this pair of mirror nuclei the theory gives two states, since one particle outside the ^{28}Si core can only be in a $2s_{\frac{1}{2}}$ or $1d_{\frac{1}{2}}$ orbit. Both states fit the experimental energies well (fig. 2A). For the other experimental levels of even parity, core excitations would have to be taken into account.

^{30}Si/P *nuclei.* The lowest states (up to 3 MeV) fit the experimental data well (fig. 2B.). The calculations show (see table 2), that the ground-state configuration of ^{30}P is mainly sd and not s^2 as might be expected. From this effect it is clear why the beta transition to the ^{30}Si ground state (mainly in an s^2 configuration) is somewhat hindered. Some low-lying levels in ^{30}P have to be ascribed to core excitations. The $J = 0$ component in the 3.8 MeV doublet in ^{30}Si is assumed to be the calculated second $J^\pi = 0^+$, $T = 1$ level. However, the calculated energy differs by 0.4 MeV from the experimental value.

^{31}S/P *nuclei.* The ground state and the levels below 3.5 MeV agree well with the experimental energies (fig. 2C). The experimental $\frac{5}{2}^+$ level at 2.23 MeV is not reproduced and thus probably originates from core excitation. The $\frac{7}{2}^+$ level at 3.41 MeV is calculated to be at 4.1 MeV. Interaction with excited core $\frac{7}{2}^+$ levels may shift the former downwards. A $J^\pi = \frac{1}{2}^+$ assignment to the 3.13 MeV level instead of $\frac{3}{2}^+$ [see ref. [4])] is experimentally much more probable [5]). This is in agreement with the calculated $\frac{1}{2}^+$ level in this region [see also ref. [6])]. Calculations by Chi and Davidson [7]), based on an asymmetric core, do not yield a second $\frac{1}{2}^+$ state below 5 MeV.

^{31}Si *nucleus.* The calculated energies for the ground state and first excited state are

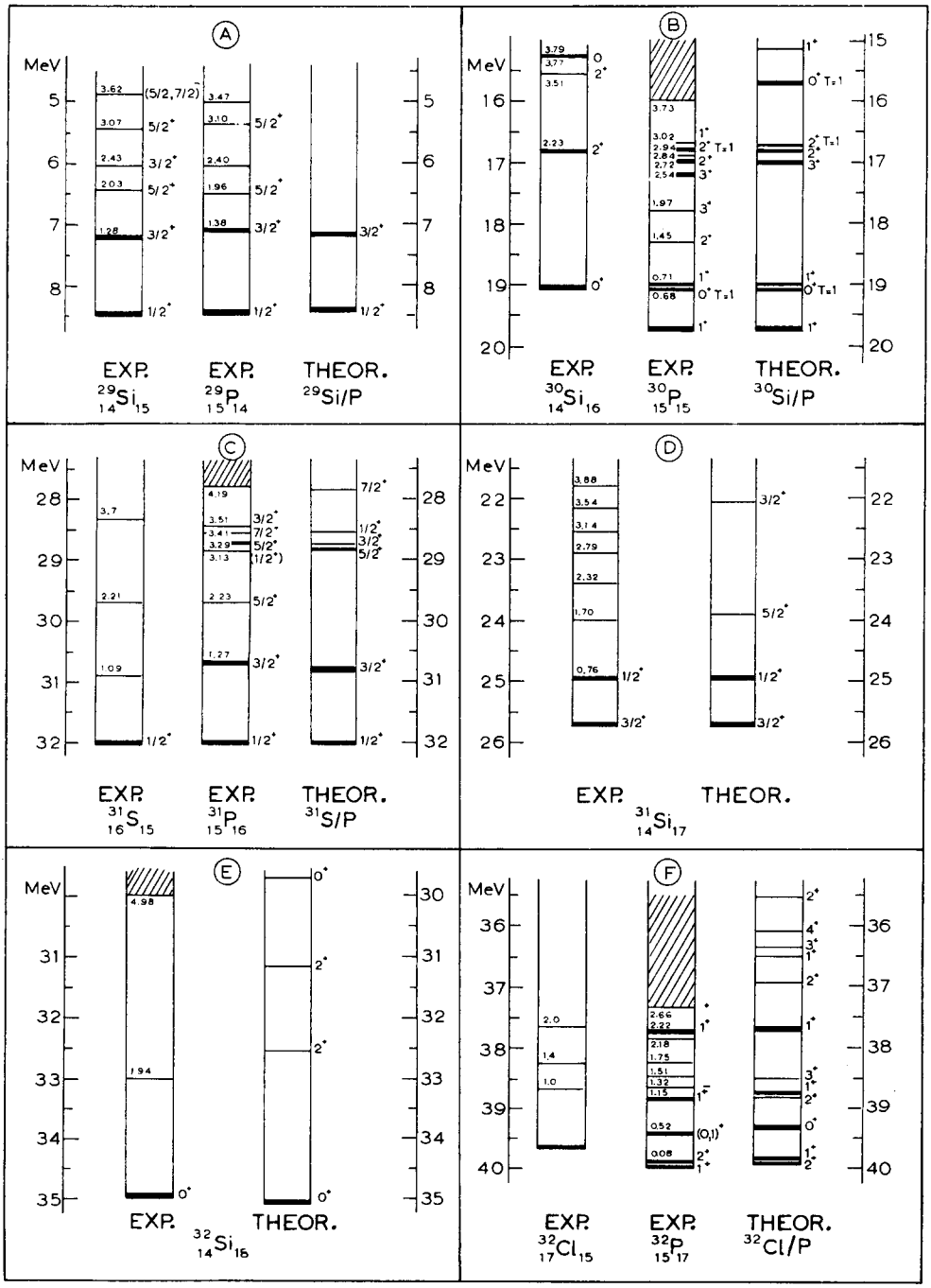

Fig. 2. Comparison of the theoretical level energies and spins with the experimental data. The levels indicated by bold lines were used in the fitting process. The vertical axis represents the excitation energy relative to the binding energy of the ^{28}Si core, with the Coulomb energy of the outer particles subtracted. Hatching indicates areas of high level density.

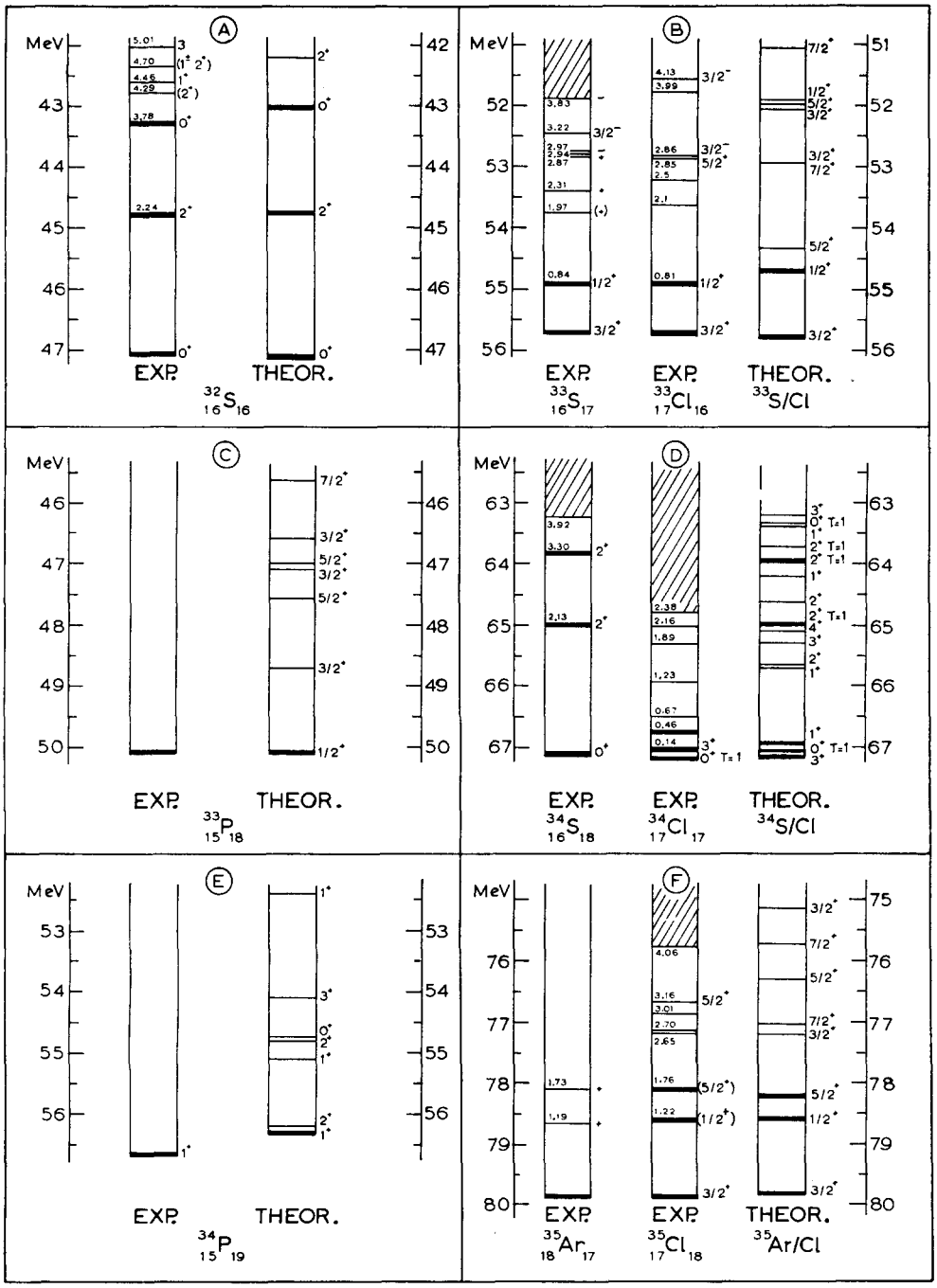

Fig. 3. See caption of fig. 2.

in good agreement with the experimental values (fig. 2D). From the calculations we expect that the 1.70 MeV level has $J^\pi = \frac{5}{2}^+$.

^{32}Si *nucleus.* Experimentally little is known about this nucleus (fig. 2E). The excitation energy of the second 2^+ level is calculated as 3.8 MeV, while from the ^{30}Si(t, p)^{32}Si reaction no levels have been reported in the 2.0–4.9 MeV region [4]).

^{32}Cl/P *nuclei.* The ground state and lowest three levels can be fitted as well as the 1^+ level at 2.22 MeV (fig. 2F). The calculations predict the level at 0.52 MeV to have $J^\pi = 0^+$. This has been confirmed by a recent investigation of the ^{31}P(n, γ)^{32}P reaction by van Middelkoop [8]). The calculated second 2^+ and lowest 3^+ levels possibly correspond with the experimental 1.51 and 1.75 MeV excited states. From the calculations we would expect, that the binding energy of ^{32}Cl should be 0.2 MeV larger. This is not unreasonable, since the experimental error is 0.3 MeV (see fig. 1).

^{32}S *nucleus.* The lowest three states show good agreement with experiment (fig. 3A). The ground-state configuration is only 50 % s^4. A third 0^+ level is predicted at 5.9 MeV (see table 2).

^{33}S/Cl *nuclei.* The ground state and first excited state agree well with experiment (fig. 3B). At 1.4 MeV a $\frac{5}{2}^+$ level is predicted. However, a recent investigation of the ^{33}S(p, p')^{33}S reaction up to $E_p = 3.2$ MeV does not show this level [9]), whereas the 0.84 and 1.97 MeV levels are strongly excited. The predicted 1.4 MeV level has neither been found in the ^{32}S(d, p)^{33}S reaction. If one assumes an inert ^{28}Si core (so that no $d_{\frac{5}{2}}$ admixture in the wave function of the 1.4 MeV level can be present), the latter reaction cannot take place due to angular momentum considerations.

^{33}P *nucleus.* Experimentally only the binding energy is known (fig. 3C). The predicted ground-state spin is $\frac{1}{2}^+$.

^{34}S/Cl *nuclei.* The lowest three states of ^{34}S and ^{34}Cl can be explained well. The calculated lowest $(J, T) = (1, 0)$ state is fitted to the level at 0.46 MeV. It is not unreasonable to expect $J^\pi = 1^+$ for this level, since it only decays to the ground state [10]). If this level is not taken along in the parameter fitting procedure, the parameters are changed in such a way, that the lowest computed 1^+ state comes out below the 0^+ and 3^+ states. The calculated doublet with spins 1^+ and 2^+ at 1.5 MeV probably corresponds to the levels experimentally found at 0.67 and 1.23 MeV (fig. 3D). Since little is known about the spins in ^{34}Cl further conclusions cannot be drawn.

^{34}P *nucleus.* The position of the ground state does not fit very well (fig. 3E). A probable explanation is the experimental uncertainty in the binding energy, amounting to 0.2 MeV.

^{35}Ar/Cl *nuclei.* The lowest levels are well explained by the theory (fig. 3F). The calculations are in favour of the spin assignments $\frac{1}{2}^+$ and $\frac{5}{2}^+$ for the first and second excited states, respectively. The configuration of the lowest $\frac{1}{2}^+$ state, which is mainly s^3d^4 instead of s^4d^3 is worthy of special mention.

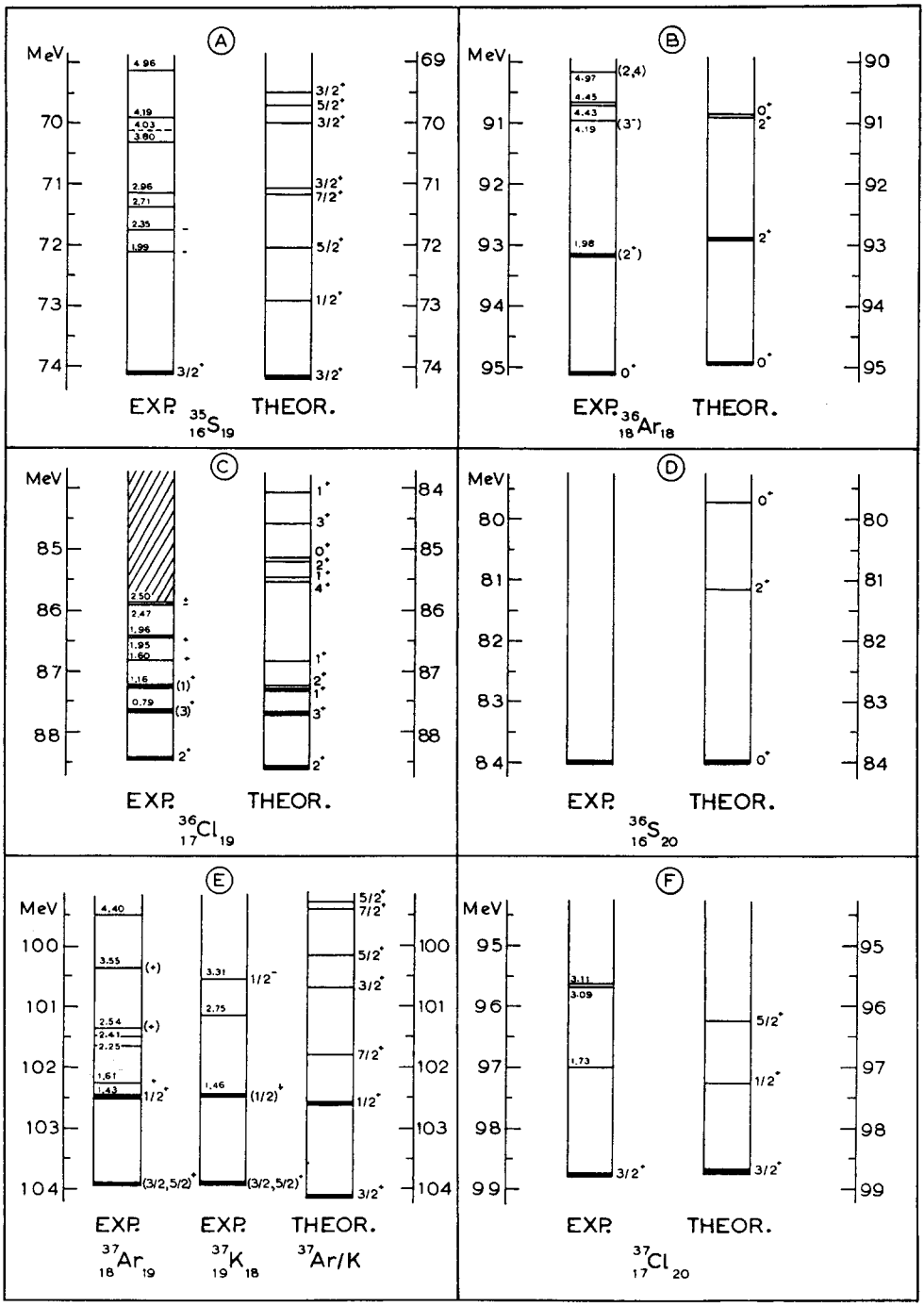

Fig. 4. See caption of fig. 2.

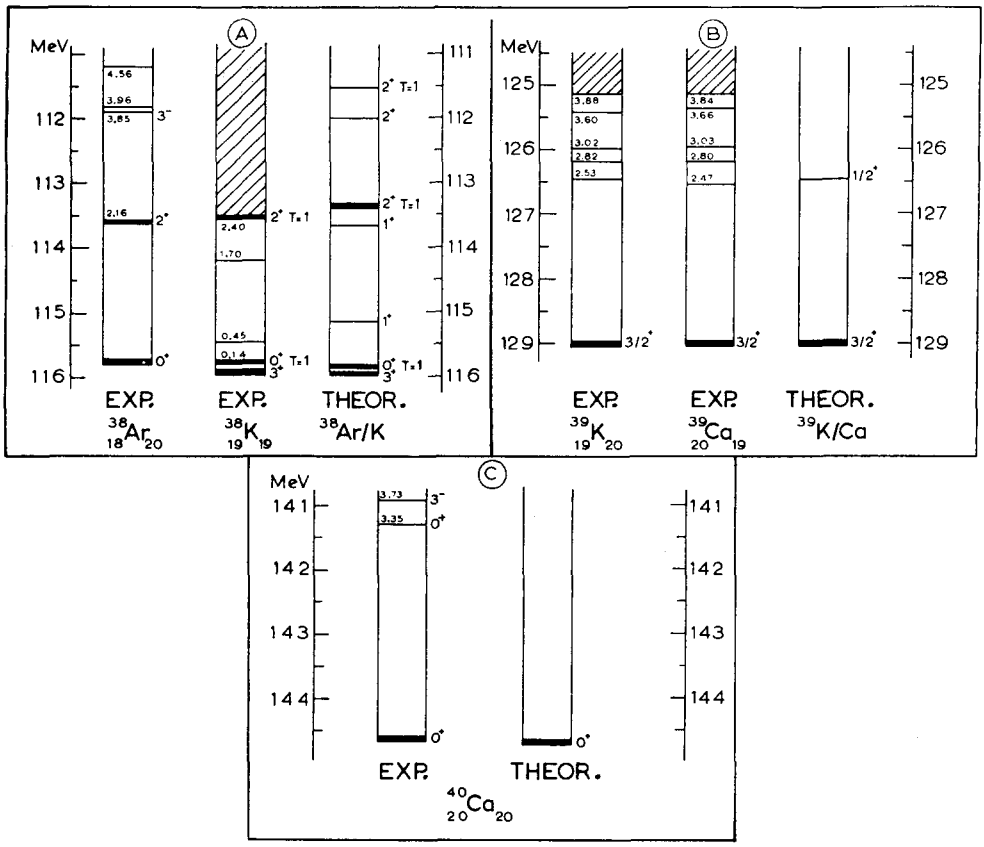

Fig. 5. See caption of fig. 2.

^{35}S *nucleus*. The calculated spin and energy of the ground state are in agreement with the experimental values (fig. 4A). The predicted $\frac{1}{2}^+$ level at 1.2 MeV may have been missed by the measurements on the ^{34}S(d, p)^{35}S reaction. The width $(2J+1)\vartheta^2$ of the transition to this level is expected to be ten times smaller than that of the already weak transition to the ^{35}S ground state (see table 3). The low-lying $\frac{5}{2}^+$ level may not have been seen in the (d, p) reaction because of angular momentum considerations (cf. discussion of ^{33}S/Cl).

^{36}Ar *nucleus*. The calculated energies of the ground state and first excited state are too high (about 0.2 MeV), although their difference is represented very well (fig. 4B). Calculations using the SU3 formalism also yield a low-lying second 0^+ level, however, below the second 2^+ level [11]).

^{36}Cl *nucleus*. The calculations confirm the spin assignments 3^+ and 1^+ to the 0.79 and 1.16 MeV levels, respectively (fig. 4C). The calculated second 2^+ and 1^+ states possibly correspond to the 1.60 and 1.95 MeV excited states. All known states in the

E_x = 2.5–4.5 MeV region have odd parity (the l_n values from the ^{35}Cl(d, p)^{36}Cl reaction are 1 or 3); however, a number of even parity levels may be expected from the present calculations.

^{36}S *nucleus.* Only the energy of the ground state can be compared with experiment and it shows good agreement (fig. 4D). The relatively high calculated excitation energy of the first 2^+ state (about 2.8 MeV) is remarkable.

^{37}Ar/K *nuclei.* A $\frac{3}{2}^+$ ground-state spin is predicted. The calculated energy and spin of the first excited state are in agreement with experiment (fig. 4E). Conclusions about the other levels cannot be made because of insufficient experimental data.

^{37}Cl *nucleus.* The calculations predict $J^\pi = \frac{1}{2}^+$ for the state at 1.73 MeV (fig. 4F).

^{38}Ar/K *nuclei.* The ground state and first excited state in both nuclei are well reproduced (fig. 5A). A recent publication on the ^{40}Ca(d, α)^{38}K reaction [12]), confirms the predicted $J^\pi = 1^+$ values for the second and third excited states in ^{38}K. It is interesting to note that the lower 1^+ level possesses mainly an s^3d^7 configuration and the higher level mainly an s^4d^6 configuration.

^{39}K/Ca *nuclei.* Only the spin of the ground state is known for this pair of mirror nuclei. The theory only yields two levels i.e., the hole-states s^{-1} and d^{-1} (cf. ^{29}P/Si). The calculated high excitation energy of the $\frac{1}{2}^+$ state is in agreement with experiment (fig. 5B).

^{40}Ca *nucleus.* For this nucleus the $2s_{\frac{1}{2}}$ and $1d_{\frac{3}{2}}$ shells are filled completely. The energy of the 0^+ ground state fits well (fig. 5C).

3. Reduced Widths for Stripping Reactions

The reduced width ϑ^2 for the stripping reaction $A+a \rightarrow (A+1)+(a-1)$, where A denotes the initial nucleus, may be written as a product of two factors [13])

$$\vartheta^2 = S\vartheta_0^2.$$

The factor S, customarily referred to as "relative reduced width" or "spectroscopic factor", is essentially an overlap integral between the final state of $A+1$ and the initial compound state of A. The "single-particle reduced width" ϑ_0^2 expresses the probability for the stripping process if the initial nucleus is considered only to provide a potential for the nucleon to be captured, i.e., the nuclear structure of the initial nucleus may be ignored. Thus, if A consists of closed shells only, one obtains $S=1$ and $\vartheta^2 = \vartheta_0^2$. The single particle reduced width ϑ_0^2 can be expressed in terms of the radial wave function of the transferred nucleon at the nuclear surface.

The nuclear structure properties of the nucleus A are contained in the spectroscopic factor S. Since the configurations of the outer shells of the nuclei in the range ^{29}Si–^{40}Ca have been determined, the spectroscopic factors S for stripping reactions on these nuclei could be calculated. The general expressions have been discussed by Macfarlane and French [13]). We shall give the results only.

TABLE 3

Calculated S factors for (d, p) and (d, n) stripping reactions

Reaction	E_x(MeV)	J^π	T	$S(l=0)$	$S(l=2)$
$^{28}Si(d,p)^{29}Si$	0.05	$1/2^+$	1/2	1.000	0
	1.27	$3/2^+$	1/2	0	1.000
$^{29}Si(d,n)^{30}P$	0.02	1^+	0	0.464	0.749
	0.67	0^+	1	1.452	0
	0.69	1^+	0	1.536	0.222
	2.73	3^+	0	0	0
	2.91	2^+	0	0	1.000
	3.00	2^+	1	0	0.943
	4.02	0^+	1	0.548	0
	4.58	1^+	0	0.000	0.028
	5.69	2^+	1	0	0.057
	5.95	1^+	1	0.000	1.000
$^{29}Si(d,p)^{30}Si$	-0.01	0^+	1	1.452	0
	2.32	2^+	1	0	0.943
	3.34	0^+	1	0.548	0
	5.01	2^+	1	0	0.057
	5.27	1^+	1	0.000	1.000
$^{30}Si(d,n)^{31}P$	-0.01	$1/2^+$	1/2	1.296	0
	1.22	$3/2^+$	1/2	0	0.813
	3.18	$5/2^+$	1/2	0	0
	3.27	$3/2^+$	1/2	0	0.076
	3.46	$1/2^+$	1/2	0.049	0
	4.15	$7/2^+$	1/2	0	0
	5.26	$3/2^+$	1/2	0	0.104
	5.60	$5/2^+$	1/2	0	0
$^{30}Si(d,p)^{31}Si$	-0.02	$3/2^+$	3/2	0	0.834
	0.76	$1/2^+$	3/2	0.274	0
	1.79	$5/2^+$	3/2	0	0
	3.65	$3/2^+$	3/2	0	0.001
	5.55	$3/2^+$	3/2	0	0.027
$^{31}P(d,p)^{32}P$	-0.11	2^+	1	0	0.752
	-0.05	1^+	1	0.023	0.593
	0.52	0^+	1	0.363	0
	1.00	2^+	1	0	0.064
	1.06	1^+	1	0.146	0.242
	1.30	3^+	1	0	0
	2.13	1^+	1	0.019	0.033
	2.88	2^+	1	0	0.004
	3.30	1^+	1	0.000	0.030
	3.46	3^+	1	0	0
	3.73	4^+	1	0	0
	4.25	2^+	1	0	0.008
$^{31}P(d,p)^{32}P$ (continued)	4.57	1^+	1	0.013	0.000
	4.68	3^+	1	0	0
	4.98	2^+	1	0	0.003
$^{31}P(d,n)^{32}S$	-0.04	0^+	0	2.819	0
	2.32	2^+	0	0	1.054
	4.06	0^+	0	0.475	0
	4.85	2^+	0	0	0.069
	5.90	0^+	0	0.003	0
	5.95	4^+	0	0	0
$^{32}S(d,p)^{33}S$	-0.08	$3/2^+$	1/2	0	0.820
	1.03	$1/2^+$	1/2	0.242	0
	1.38	$5/2^+$	1/2	0	0
	2.77	$7/2^+$	1/2	0	0
	2.77	$3/2^+$	1/2	0	0.013
	3.65	$3/2^+$	1/2	0	0.002
	3.74	$5/2^+$	1/2	0	0
	3.83	$1/2^+$	1/2	0.010	0
	4.67	$7/2^+$	1/2	0	0
	4.97	$3/2^+$	1/2	0	0.007
	5.34	$9/2^+$	1/2	0	0
	5.64	$5/2^+$	1/2	0	0
$^{33}S(d,n)^{34}Cl$	0.02	3^+	0	0	1.553
	0.04	0^+	1	0	2.010
	0.22	1^+	0	0.277	0.215
	1.47	1^+	0	0.006	0.869
	1.49	2^+	0	0.124	0.012
	1.86	3^+	0	0	0.087
	2.05	4^+	0	0	0
	2.17	2^+	1	0.000	0.803
	2.53	2^+	0	0.152	0.000
	2.98	1^+	0	0.000	0.511
	3.21	2^+	1	0.014	0.562
	3.44	2^+	1	0.106	0.271
	3.81	1^+	0	0.000	0.026
	3.82	0^+	1	0	0.002
	3.97	3^+	0	0	0.007
	4.97	1^+	1	0.117	0.017
	5.03	3^+	0	0	0.018
	5.16	0^+	1	0	0.046
	5.32	3^+	1	0	0.007
	5.43	5^+	0	0	0
	5.47	4^+	1	0	0
	5.73	2^+	1	0.030	0.000
	5.97	2^+	0	0.000	0.002

Let the wave function of the target nucleus A be given by $\Phi[A] = \sum_i a_i \varphi\{s_{\alpha_i}^{n_i} d_{\beta_i}^{m_i} | \Gamma_A\}$ (the Greek letters denote (J, T) pairs; see I) and the wave function of the final nucleus by $\Psi[A+1] = \sum_j b_j \psi\{s_{\gamma_j}^{n_j} d_{\varepsilon_j}^{m_j} | \Gamma_{A+1}\}$. The S factor for $l = 0$ capture is then given by the overlap integral †

$$S(l=0) = [\sum_{ij} (-1)^{\alpha_i - \gamma_j} a_i b_j (n_j)^{\frac{1}{2}} \langle s^{n_j} \gamma_j | s^{n_i} \alpha_i \rangle U(s\alpha_i \Gamma_{A+1} \varepsilon_j; \gamma_j \Gamma_A) \delta(m_i, m_j) \delta(n_i, n_j - 1) \delta(\beta_i, \varepsilon_j)]^2.$$

† See eqs. (III. 59, 64, 67, 83) of ref. [13]).

TABLE 3
(continued)

Reaction	E_x(MeV)	J^π	T	S(l=0)	S(l=2)	Reaction	E_x(MeV)	J^π	T	S(l=0)	S(l=2)
$^{33}S(d,p)^{34}S$	0.04	0^+	1	0	2.010	$^{35}Cl(d,n)^{36}Ar$	4.20	2^+	0	0.140	0.692
	2.17	2^+	1	0.000	0.803	(continued)	5.69	4^+	0	0	0
	3.21	2^+	1	0.014	0.562						
	3.44	2^+	1	0.106	0.271	$^{35}Cl(d,p)^{36}Cl$	-0.17	2^+	1	0.002	0.940
	3.82	0^+	1	0	0.002		0.72	3^+	1	0	0.240
	4.97	1^+	1	0.117	0.017		1.16	1^+	1	0.048	0.005
	5.16	0^+	1	0	0.046		1.22	2^+	1	0.050	0.002
	5.32	3^+	1	0	0.007		1.61	1^+	1	0.020	0.220
	5.47	4^+	1	0	0		2.88	4^+	1	0	0
	5.73	2^+	1	0.030	0.000		2.96	1^+	1	0.006	0.037
							3.24	2^+	1	0.029	0.006
$^{34}S(d,n)^{35}Cl$	0.06	$3/2^+$	1/2	0	1.099		3.30	0^+	1	0	0.015
	1.26	$1/2^+$	1/2	0.215	0		3.84	3^+	1	0	0.001
	1.67	$5/2^+$	1/2	0	0		4.37	1^+	1	0.013	0.015
	2.65	$3/2^+$	1/2	0	0.001		4.60	3^+	1	0	0.000
	2.82	$7/2^+$	1/2	0	0		4.89	2^+	1	0.000	0.001
	3.55	$5/2^+$	1/2	0	0						
	4.11	$7/2^+$	1/2	0	0	$^{36}Ar(d,p)^{37}Ar$	-0.23	$3/2^+$	1/2	0	0.460
	4.70	$3/2^+$	1/2	0	0.004		1.32	$1/2^+$	1/2	0.069	0
	5.12	$5/2^+$	1/2	0	0		2.12	$7/2^+$	1/2	0	0
	5.15	$3/2^+$	1/2	0	0.010		3.21	$3/2^+$	1/2	0	0.004
	5.20	$1/2^+$	1/2	0.001	0		3.75	$5/2^+$	1/2	0	0
	5.35	$9/2^+$	1/2	0	0		4.50	$7/2^+$	1/2	0	0
	5.81	$5/2^+$	1/2	0	0		4.62	$5/2^+$	1/2	0	0
							5.47	$1/2^+$	1/2	0.003	0
$^{34}S(d,p)^{35}S$	-0.09	$3/2^+$	3/2	0	0.440		5.78	$3/2^+$	1/2	0	0.000
	1.18	$1/2^+$	3/2	0.113	0						
	2.07	$5/2^+$	3/2	0	0	^{36}S (d,n)^{37}Cl	0.07	$3/2^+$	3/2	0	1.136
	2.92	$7/2^+$	3/2	0	0		1.49	$1/2^+$	3/2	0.178	0
	3.04	$3/2^+$	3/2	0	0.000		2.53	$5/2^+$	3/2	0	0
	4.10	$3/2^+$	3/2	0	0.000		4.94	$3/2^+$	3/2	0	0.000
	4.38	$5/2^+$	3/2	0	0						
	4.58	$3/2^+$	3/2	0	0.001	$^{37}Cl(d,n)^{38}Ar$	-0.17	0^+	1	0	2.594
	5.47	$1/2^+$	3/2	0.000	0		2.37	2^+	1	0.020	0.133
	5.71	$5/2^+$	3/2	0	0		4.21	2^+	1	0.006	0.001
	5.80	$1/2^+$	3/2	0.002	0						
	5.95	$7/2^+$	3/2	0	0	$^{38}Ar(d,n)^{39}K$	0.04	$3/2^+$	1/2	0	0.713
							2.56	$1/2^+$	1/2	0.080	0
$^{35}Cl(d,n)^{36}Ar$	0.21	0^+	0	0	3.889						
	2.23	2^+	0	0.002	1.442	^{39}K (d,n)^{40}Ca	-0.04	0^+	0	0	8.000
	4.20	0^+	0	0	0.026						

The value $S = 0$ denotes that the stripping reaction is impossible due to angular momentum relations (with the assumption of only $2s_{\frac{1}{2}}$ and $1d_{\frac{3}{2}}$ nucleons taking part in the stripping process); $S = 0.000$ indicates that the computed value is smaller than one unit of the last decimal.

(The notation for the coefficient of fractional parentage and the normalized Racah coefficient is the same as in I.) The S factor for $l = 2$ capture is given by †

$$S(l=2) = [\sum_{ij} a_i b_j (m_j)^{\frac{1}{2}} \langle d^{m_j} \varepsilon_j | d^{m_i} \beta_i \rangle U(d\beta_i \Gamma_{A+1} \gamma_j; \varepsilon_j \Gamma_A) \delta(n_i, n_j) \delta(m_i, m_j - 1) \delta(\alpha_i, \gamma_j)]^2.$$

† See eqs. (III. 59, 64, 67, 83) of ref. [13]).

In table 3 the S factors are listed for the (d, p) and (d, n) reactions on stable nuclei in the region $28 \leqq A < 40$ (levels above 6 MeV are left out).

Only relatively few experimental data on stripping widths are available for comparison with our theoretical predictions. In table 4 we have listed all values of ϑ^2, that

TABLE 4

Theoretical and experimental reduced widths for stripping reactions

Reaction	Theoretical				Experimental					
	E_x (MeV)	$J\pi$	$S\vartheta_0^2 \times 10^3$ $l=0$	$l=2$	E_x	$J\pi$	$\vartheta^2_{absolute} \times 10^3$ $l=0$	$l=2$	$\vartheta^2_{relative}$ $l=0$	$l=2$
^{28}Si(d, p)^{29}Si	0.05	$\frac{1}{2}^+$	25	0	0	$\frac{1}{2}^+$	21	—	25	—
	1.27	$\frac{3}{2}^+$	0	15	1.28	$\frac{3}{2}^+$	—	14	—	17
^{28}Si(d, n)^{29}P	0.05	$\frac{1}{2}^+$	25	0	0	$\frac{1}{2}^+$	17	—	25	—
	1.27	$\frac{3}{2}^+$	0	15	1.38	$\frac{3}{2}^+$	—	9	—	13
^{29}Si(d, p)^{30}Si	−0.01	0^+	36	0	0	0^+			36	—
	2.32	2^+	0	14	2.23	2^+			—	24
^{30}Si(d, p)^{31}Si	−0.02	$\frac{3}{2}^+$	0	13	0	$\frac{3}{2}^+$			—	13
	0.76	$\frac{1}{2}^+$	7	0	0.76	$\frac{1}{2}^+$			7	—
^{31}P(d, p)^{32}P	−0.05	1^+	0.6	9	0	1^+			0.6	9
	−0.11	2^+	0	11	0.08	2^+			—	8
	0.52	0^+	9	0	0.52	0^+			6	—
	1.00	2^+	0	1	1.51 [a])	—			—	—
	1.06	1^+	4	4	1.15	1^+			4	—
	1.30	3^+	0	0	1.75 [a])	—			—	—
	2.13	1^+	0.5	0.5	2.23	1^+			1	4
^{31}P(d, n)^{32}S	−0.04	0^+	70	0	0	0^+	6	—	70	—
	2.32	2^+	0	16	2.24	2^+	—	3	—	35
^{32}S(d, p)^{33}S	−0.08	$\frac{3}{2}^+$	0	12	0	$\frac{3}{2}^+$	—	25	—	12
	1.03	$\frac{1}{2}^+$	6	0	0.84	$\frac{1}{2}^+$	16	—	7	—
^{35}Cl(d, p)^{36}Cl	−0.17	2^+	0.05	14	0	2^+	0.4	8	0.7	14
	0.72	3^+	0	4	0.79	(3^+)	—	2	—	4
	1.16	1^+	1.2	0.08	1.16	(1^+)	1.8	2	3	4
	1.22	2^+	1.3	0.03	1.60 [a])	—	0.5	—	0.9	—

[a]) These cases are dubious because experimentally the spins are unknown, while the experimental and calculated energies agree rather badly.

could be obtained in the region of interest. These reduced widths, taken from ref. [4]), were extracted from the measured differential cross-sections of stripping reactions (and of pick-up reactions that will not be considered here, but are described by very analogous expressions, being the inverse of the stripping process). Expressions for the differential cross-sections in terms of the reduced width ϑ^2 in the Born approximation can be found in ref. [13]).

From Macfarlane and French the following values were taken for the single particle reduced widths in the $2s_{\frac{1}{2}}$ and $1d_{\frac{3}{2}}$ shells: $\vartheta_0^2(2s_{\frac{1}{2}}) = 0.025$ and $\vartheta_0^2(1d_{\frac{3}{2}}) = 0.015$, respectively. Thus with the spectroscopic factors S of table 3, the theoretical widths

$S\vartheta_0^2$ were calculated. The results are also given in table 4. As is seen in table 4 not all reduced widths are known in absolute measure. The experimental relative values of ϑ^2 for each reaction have been normalized to the computed reduced width of the strongest component in the ground-state transition. Taking into account the uncertainties in the values of ϑ_0^2 and in the experimental values of the reduced widths, one observes that rather good agreement is obtained between the predicted values of $S\vartheta_0^2$ and the measured values of ϑ^2.

4. Concluding Remarks

The possibility of describing all two-particle interactions of the $2s_{\frac{1}{2}}\,1d_{\frac{3}{2}}$ shell in terms of only seventeen parameters, has led us to extract the values of these parameters from experimental data and to calculate the configurations of the nucleons in this shell. With the parameters many more nuclear levels could be predicted than were used for the determination of the parameters. Most of these predicted level energies were in the neighbourhood of measured levels, of which the spins were unknown.

The close correspondence between the four low-lying levels (given by the (J, T) values (0, 1), (1, 0), (2, 1) and (3, 0)) in ^{34}S/Cl and ^{38}Ar/K, suggests the applicability of particle-hole relations between the configurations s^4d^2 and s^4d^{-2}. Inspection of the calculated configurations (see table 2) shows, however, that these four nuclear levels are by no means pure (except for the ground states of ^{38}Ar and ^{38}K) and thus the use of simple particle-hole considerations in these nuclei is not justified.

It is rather striking, that the "centre of gravity" [14]) of the first and second excited states in ^{29}P/Si is 1.8 MeV, which is just the energy of the first 2^+ level of the ^{28}Si core. It should be noted that for the "centre of gravity" considerations in ^{29}P/Si, it is assumed that an *excited* 2^+ core couples with the extra nucleon in a $2s_{\frac{1}{2}}$ orbit. In the present calculations, however, an *inert* core is employed to produce the lowest $\frac{3}{2}^+$ level of ^{29}P/Si. Omission of this state in the fitting procedure caused a negligible effect on the values of the parameters.

A calculation of gamma-transition probabilities, in which the computed nuclear configurations are utilized, is in progress. Similarly, it should be possible to apply these configurations in calculations of beta-transition probabilities and magnetic moments. It may be expected that the agreement with experiment will be less good than for the stripping reactions, where the outer nucleons play a predominant role.

In this paper the nuclear interactions of all two-particle configurations in the $2s_{\frac{1}{2}}\,1d_{\frac{3}{2}}$ shell were determined. It would be interesting to investigate the requirements for the effective nuclear forces that will reproduce these two-particle matrix elements.

Helpful discussions with Professor P. M. Endt and Dr. C. van der Leun are gratefully acknowledged. We would like to thank the staffs of the Mathematical Center in Amsterdam and the Mathematical Institute in Utrecht for computing facilities.

This investigation was partly supported by the joint program of the "Stichting voor Fundamenteel Onderzoek der Materie" and the "Nederlandse Organisatie voor Zuiver Wetenschappelijk Onderzoek".

References

1) P. W. M. Glaudemans, G. Wiechers and P. J. Brussaard, Nuclear Physics **56** (1964) 529
2) A. Arima, Progr. Theor. Phys. **19** (1958) 421
3) F. Everlingh, L. A. König, J. H. E. Mattauch and A. H. Wapstra, Nuclear Physics **18** (1960) 529
4) P. M. Endt and C. van der Leun, Nuclear Physics **34** (1962) 1
5) H. van Rinsvelt, private communication
6) C. Broude, L. L. Green and J. C. Willmott, Proc. Phys. Soc. **A72** (1958) 1122
7) B. E. Chi and J. P. Davidson, Phys. Rev. **131** (1963) 366
8) G. van Middelkoop, private communication
9) C. van der Leun and P. M. Endt, Nuclear Physics **53** (1964) 540
10) P. W. M. Glaudemans, L. Eriksson and J. A. R. Werkhoven, Nuclear Physics **55** (1964) 559
11) J. P. Elliott, Selected topics in nuclear theory, ed. by F. Janouch (International Atomic Energy Agency, Vienna, 1963) p. 198
12) J. Jänecke, Nuclear Physics **48** (1963) 129
13) M. H. Macfarlane and J. B. French, Revs. Mod. Phys. **32** (1960) 567
14) A. de-Shalit, Phys. Rev. **122** (1961) 1530